



# Static Bending Solutions for an Isotropic Rectangular Clamped/Simply Supported Plates Using 3-D Plate Theory

Festus Chukwudi Onyeka <sup>a</sup>, Chidobere David Nwa-David <sup>b</sup>, Benjamin Okwudili Mama <sup>c,\*</sup>

<sup>a</sup> Department of Civil Engineering, Edo State University Uzairue, Edo State, 312102, Nigeria.

<sup>b</sup> Department of Civil Engineering, Michael Okpara University of Agriculture, Umudike, Abia State, 440109, Nigeria

<sup>c</sup> Department of Civil Engineering, University of Nigeria, Nsukka, Enugu State, 410101, Nigeria.

## Abstract

The A polynomial displacement function was applied with three-dimensional (3-D) elasticity theory to solve the bending problem of isotropic rectangular thick plate that is simply-supported at the first and fourth edges, clamped and free on the second-third edges (SCFS). In the analysis, the model addressed the effect of shear deformation as well as the transverse normal strain-stress, obviating the coefficients of shear correction. The 3-D kinematic and constitutive relations were used to formulate the total potential energy expression, thereafter, the equilibrium equation developed from the energy functional transformation was used to get the relationship for slope and deflection. The solution of the equilibrium equation birthed the exact polynomial deflection function while the coefficient of deflection of the plate was produced from the governing equation using direct variation approach. These solutions were employed to analyze the bending characteristics of the SCFS rectangular plate by establishing the expression for calculating the displacement and stresses of the plate. The outcome of this study certifies that solutions from 3D model is exact and safe compared to refined plate theories applied by previous authors. Compared with the 3-D plate analysis, the percentage differences presented are as close as 2.9% and 3.7% for all span-to-thickness ratios. The comprehensive average percentage variation of the center deflection values obtained by Onyeka *et al.*, (2020) and Gwarah (2019), is 0.39%. This revealed that at the 99.7 % confidence level, the 3-D plate theory is most suitable and reliable for studying the bending characteristics of thick plates.

**Keywords:** SCFS thick plate, 3D plate theory, Polynomial displacement shape function, Variation technique, Exact solution

## 1. Introduction

Three-dimensional Plates are widely applied in naval, aeronautical, mechanical, geotechnical and structural engineering for modelling bridge deck slabs, turbine disks, water tanks, ship hulls, retaining walls, machine parts, architectural structures etc. [1-4] as they are three dimensional structural elements with spatial dimensions along x, y, and z axes, whose thickness dimension is much lesser compared to the other two parallel in-plane dimensions [5, 6].

Plates can be non-homogeneous, homogeneous, orthotropic, anisotropic, or isotropic based on their material

---

\* Corresponding Author: ORCID: <https://orcid.org/0000-0002-2668-9753>; Email: [boniface.mama@unn.edu.ng](mailto:boniface.mama@unn.edu.ng)

constituents [7-9]. With respect to shapes, they can be quadrilateral, square, circular, or rectangular. Free, simply supported and fixed conditions are different forms of edges of plates. Considering their thickness, they are either thin, moderately thick or thick [10-12]. In Refs. [13, 14], rectangular plates whose span-to-thickness ratio ( $a/t$ ) lies between 45 and 100, 20 and 45, and less than 20 are regarded as thin, moderately-thick and thick plates respectively. In engineering works, the demand for thick plates is on the increase because of its economic benefits, load resistance capacity, high strength and light weight properties [15-17].

The plate structure is generally analyzed in terms of vibration, buckling and bending [12, 18]. The application of lateral loads or external forces on the plate often result to bending, which is the deformation of the structure perpendicular to its surface. Deformation is increased when the critical load is exceeded by the induced load [19]. Consequently, the plate fails. Practical attention and accurate solution are required in order to defeat failure occurrence. Hence, this bending study is necessary.

Different scholars have developed and used diverse theories such as the classical plate theory (CPT), refined plate theories (RPTs), and three-dimensional theory (3-D); to describe the bending behavior of thick plates. The uncompounded Kirchhoff plate theory (CPT) [20] is considered inadequate for determining the bending solution of thick plates since it neglects transverse shear effects. RPTs which consists of the First Order Shear deformation Theory (FSDT) [21, 22], Trigonometric Shear deformation Theory (TSDT) [23, 24], Exponential Shear deformation Theory (ESDT) [24], Polynomial Shear deformation Theory (PSDT) [25, 26] and the Higher Order Shear deformation Theory (HSDT) [27, 28]; gives a better but incomplete solution in the thick plate analysis. While FSDTs (Reissner-Mindlin theory) applies correction factors, HSDTs without it, satisfies the zero shear-stress conditions at the top and underside of the plates.

RPTs are inconsistent and also addressed as 2-D plate theory as they overlook the normal stress and strain along the thickness axis of the plate. These 2-D solutions are inaccurate and unreliable. The beauty of the 3-D solution is its comprehensive system of fifteen governing equations which consists of material constitutive laws of generalized stress - strain equations, the kinematic relations for six strains and displacements and the three differential equations of equilibrium [13, 29-34]. Since thick plate analysis is basically a three-dimensional problem, this model is needful and it is a plus for evaluating thick plates with SCFS support status.

Assessment on bending can be done analytically, numerically or with an energy approach or a miscellany of any [29]. In analytical approach, the solution of the bending problem, fulfils the boundary requirements of the plate in the governing equations at different positions of the plate surface. This method includes; Integral transform, Eigen expansion, Navier and Levy series [35], while numerical approach whose solutions are approximate [36-38], consists of; Galerkin, Collocation, Bubnov-Galerkin, truncated double Fourier series, Kantorovich methods, boundary element, Ritz, and finite difference. The energy method whose total energy is equivalent to the total of strain and potential energy or external work on the continuum; can take an analytical or a numerical form.

Analytical-energy approach with 3-D model is used in this paper to evaluate the displacements (in-plane and out-of-plane), moments, and all the stresses at different points of plates with SCFS boundary order, considering the effect of aspect ratios, with the application of exact polynomial displacement-shape function. Contrary to preceding works, this study covers the deflection, shear stresses at x-y axis, x-z axis, y-z axis, the normal stresses along x, y, z co-ordinates produced due to the applied load on the plate, and the in-plane displacement in the direction of x and y co-ordinates. Many authors applied assumed displacement-shape functions to solve plate bending which led to inexact solutions. The integrity and accuracy of solutions to the thick plate bending problem are determined by the quality of shape functions used during the analysis and this is a matter of great concern for engineers. This gap is also bridged in this study.

The excellency of this work is that its displacement function are exactly as they are obtained from the governing equations employing an analytical approach, coupled with the use of polynomial functions whose differentiation and integration are quite easy, accurate and can be successfully applied to solve thick rectangular plate of any support-condition. Worthy to note is that previous scholars were not able to extensively address the bending behaviour of SCFS-plate configuration neither did they do justice to the application of 3-D models. This study covered the gap.

Ghugal and Sayyad [39] presented bi-directional bending of thick plates using TSDT to address the effects of transverse-normal strain and shear deformation with cosine and sinusoidal function respectively. The virtual work principle was employed to obtain the support conditions and governing equations of the model. TSDT was also applied by [28] but with Navier's solution technique to obtain an analytical solution for isotropic thick plates. The effect of transverse shear was also factored into their study. Although their work satisfied the shear-stress free surface conditions without the aid of shear correction factor, the study was not three-dimensional and polynomial functions were not considered.

The precept of virtual work and HSDT was employed by Mantari and Soares [40] and was confirmed to be accurate when compared with other RPTs. The authors obtained a Navier-type analytically-solution of the governing equations of simply supported plates subjected to transverse bi-sinusoidal loads, with an assumption of variation in

the mechanical features of the plates in the thickness axis. Thick plates with SCFS support order under uniformly distributed loads, were not addressed. The 3-D plate theory was also not applied.

A polynomial shape function with the direct variation energy approach and 2-D theory was applied by [41] to obtain the displacement coefficients for CCCS and SSFS plates, without the need for correction factor. The authors failed to cover SCFS plates. The three-dimensional plate elasticity model was not considered.

A new inverse TSDT was applied by [42] to develop a finite element solution for bi-directional bending assessment of thick isotropic plates. They authors considered transverse shear deflection and rotating inertia effects. Dynamic version of the virtual work principle was used to get the dominant equations and edge conditions of the theory. When compared with previous HSDTs, their model yielded precise predictions of stresses and displacements. They didn't carry out a three-dimensional investigation. Polynomial functions and SCFS thick plates were not considered.

An exact polynomial functions obtained from the governing equation with an analytical approach were used by [43] to analyze SSSS 3-D thick plates. The authors obtained the total potential-energy functional using the six strains and stress components. The coarseness of RPT for thick plate analysis was divulged, when their solution was set side by side with those of RPT. However, they failed to cover SCFS thick plates.

A numerical approach based on the 3-D theory was used by [44] to get the bending solutions of a thick plate. They applied Spline-collocation method with two-coordinate directions. The displacements and stresses in clamped plates were determined. The deflection value at any given point in the plate cannot be properly examined from by their approach. Plates with CSFS edge condition were not taken into consideration.

Onyeka *et al.* [45] developed 3D trigonometric models for analyzing thick plates bending effects using the energy method. In [45], clamped thick plates were considered. The solution of their study confirmed the excellency of 3D theory in the thick plate analytic investigation. But both authors failed to analyze the bending attributes of SCFS plates. Polynomial displacement function was not taken into account.

In Refs. [46-88] applied non-classical elasticity theories to investigate the behavior of plates, but their studies were centered on functionally graded material. Their attention was more on nanostructures using nonlocal elasticity, strain gradient and nonlocal strain gradient theory. These authors failed to examine the bending attributes. Their study failed to capture isotropic rectangular plates. They were not able to consider the three-dimensional plate theory and SCFS boundary terms.

Previous scholars who employed refined 2-D theories for analyzing isotropic rectangular plates, made erroneous assumptions with respect to deformation kinematics and inexact bending solutions were obtained. Very few researchers considered the 3-D model and this gap is addressed in this study.

Safe and cost-effective analysis were not achieved by most antecedent scholars in their study due to the application of assumed displacement shape functions. To avert laborious mathematical analysis, these functions were not derived from the governing equilibrium equation. This research work covers this gap as it employs the exact displacement function to obtain its closed-form solution for the thick plate bending analysis.

Although several authors have carried out studies on the bending of rectangular plates, their solutions were approximate as they failed to address all the stress elements as well as their inability to satisfy exactly the specified conditions of the edges or the governing differential equation or both. To conquer the limitations of previous works, a complete 3-D plate theory is applied in this study. This work determines the stresses and displacements of SCFS isotropic rectangular plates using exact polynomial shape functions.

The physical interpretation of SCFS plate is that, the clamped edge is supported by a beam and continuous over the span of the plate, the other two edges are supported by a roller while the remaining one is free of support i.e. hang without support (Eg. Cantilever). This makes the study very significant because such boundary condition (BC) exist depending on the type of roller, beam or column support in the plate structure, thus, whenever such BC occurs it ought to be analysed a such to ensure that it account for all the forces (stresses) acting on it. This is because, forces are generated due to the applied load on the structure thereby will introduce significant errors in the result if they account for. Hence, the essence of the case study.

## 2. Methodology

### 2.1. Model Formulation

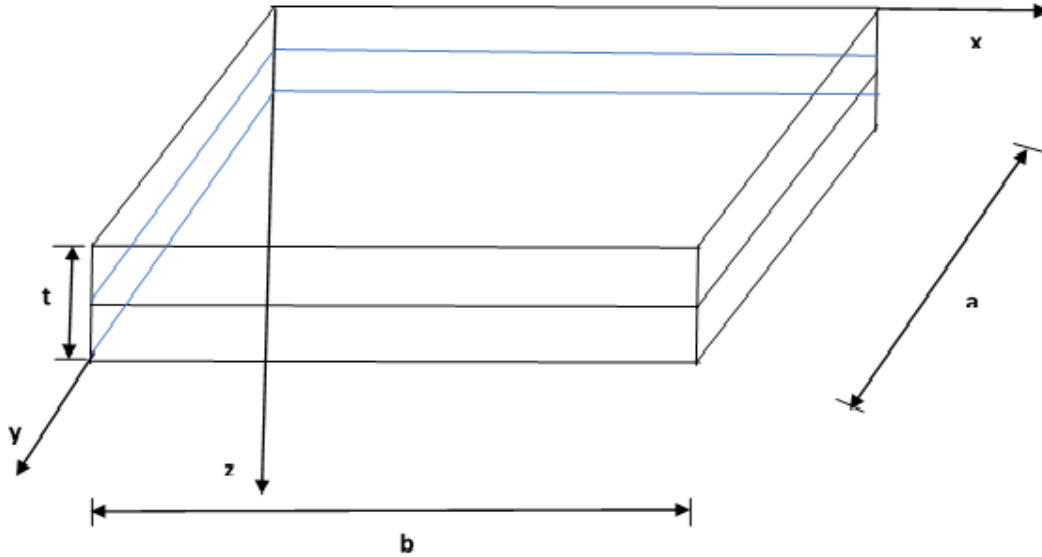


Fig. 1: An element of thick rectangular plate showing middle surface

The research methodology of this study is presented by considering a rectangular plate in the Figure 1 as a three-dimensional element in which the deformation exists in the three axis: length (a), width (b) and thickness (t). The length, width and thickness of the plate is along the x, y and z axis of the plate respectively. The analytical approach of energy method was used to obtain formulas for the analysis. The 3-D kinematics and constitutive relations for a static elastic theory of plate was used to formulate the governing equations which enables development of the formulae for the analysis.

### 3.2. Kinematics

The kinematics of the study if formulated by taking the assumption of the plate that the x-z section and y-z section, is no longer normal to x-y plane after bending. Thus, the 3-D displacement kinematics along x, y and z axis are obtained in line as:

$$p = z \cdot \phi_x \quad (1)$$

$$q = z \cdot \phi_y \quad (2)$$

Given that:

$$z = kt \quad (3)$$

$$\beta = \frac{a}{t} \quad (4)$$

$$\gamma = \frac{b}{a} \quad (5)$$

Thus, the six non-dimensional coordinates strain components were derived using strain-displacement expression according to Hooke's law and presented in Equation (6) - (11):

$$\varepsilon_x = \frac{1}{a} \cdot \frac{\partial p}{\partial u} \quad (6)$$

$$\varepsilon_y = \frac{1}{a\gamma} \cdot \frac{\partial q}{\partial v} \quad (7)$$

$$\varepsilon_z = \frac{1}{t} \cdot \frac{\partial U}{\partial k} \quad (8)$$

$$\gamma_{xy} = \frac{1}{a} \cdot \frac{\partial q}{\partial u} + \frac{1}{a\gamma} \cdot \frac{\partial p}{\partial v} \quad (9)$$

$$\gamma_{xz} = \frac{1}{a} \cdot \frac{\partial U}{\partial u} + \frac{1}{t} \cdot \frac{\partial p}{\partial k} \quad (10)$$

$$\gamma_{yz} = \frac{1}{a\gamma} \cdot \frac{\partial U}{\partial v} + \frac{1}{t} \cdot \frac{\partial q}{\partial k} \quad (11)$$

### 2.3. Constitutive Relations

The three dimensional constitutive relation for isotropic material is given as:

$$\begin{bmatrix} \varepsilon_x \\ \varepsilon_y \\ \varepsilon_z \\ \gamma_{xz} \\ \gamma_{yz} \\ \gamma_{xy} \end{bmatrix} = \frac{1}{E} \begin{bmatrix} 1 & -\mu & -\mu & 0 & 0 & 0 \\ -\mu & 1 & -\mu & 0 & 0 & 0 \\ -\mu & -\mu & 1 & 0 & 0 & 0 \\ 0 & 0 & 0 & 2(1+\mu) & 0 & 0 \\ 0 & 0 & 0 & 0 & 2(1+\mu) & 0 \\ 0 & 0 & 0 & 0 & 0 & 2(1+\mu) \end{bmatrix} \begin{bmatrix} \sigma_x \\ \sigma_y \\ \sigma_z \\ \tau_{xz} \\ \tau_{yz} \\ \tau_{xy} \end{bmatrix} \quad (12)$$

The six stress components were obtained by substituting Equations 6 to 11 into Equation 12 and simplifying the outcome gave:

$$\sigma_x = \left[ \mu \frac{kt}{\gamma a} * \frac{\partial \phi_y}{\partial v} + (1 - \mu) \frac{kt}{a} * \frac{\partial \phi_x}{\partial u} + \mu \frac{1}{t} * \frac{\partial U}{\partial k} \right] \frac{E}{(1 + \mu)(1 - 2\mu)} \quad (13)$$

$$\sigma_y = \left[ \mu kt * \frac{\partial \phi_x}{a \partial u} + \frac{\mu}{t} * \frac{\partial U}{\partial k} + \frac{(1 - \mu)kt}{\gamma a} * \frac{\partial \phi_y}{\partial v} \right] \frac{E}{(1 + \mu)(1 - 2\mu)} \quad (14)$$

$$\sigma_z = \left[ \frac{\mu kt}{\gamma a} * \frac{\partial \phi_y}{\partial v} + \frac{(1 - \mu)}{t} * \frac{\partial U}{\partial k} + \mu kt * \frac{\partial \phi_x}{a \partial u} \right] \frac{E}{(1 + \mu)(1 - 2\mu)} \quad (15)$$

$$\tau_{xy} = \left[ \frac{kt \partial \phi_y}{a 2 \partial u} * \frac{kt}{2 \gamma a} \frac{\partial \phi_x}{\partial v} \right] \frac{E(1 - 2\mu)}{(1 + \mu)(1 - 2\mu)} \quad (16)$$

$$\tau_{yz} = \left[ \frac{1}{a 2 \gamma} \frac{\partial U}{\partial Q} + \frac{\phi_y}{2} \right] \frac{(1 - 2\mu)E}{(1 + \mu)(1 - 2\mu)} \quad (17)$$

$$\tau_{xz} = \left[ \frac{1}{a} \frac{\partial U}{2 \partial u} + \frac{\phi_x}{2} \right] \frac{(1 - 2\mu)E}{(1 + \mu)(1 - 2\mu)} \quad (18)$$

### 2.4. Formulation of Energy

The potential energy which is summation of all the external work done on the body of the material and strain energy generated due to the applied load on the plate is mathematically defined as:

$$\Xi = \epsilon - \omega \quad (19)$$

Given that;

$$\Xi = wab \int_0^1 \int_0^1 C du dv \quad (20)$$

And;

$$\epsilon = \frac{tab}{2} \int_0^1 \int_0^1 \int_{-0.5}^{0.5} (\sigma_x \epsilon_x + \sigma_y \epsilon_y + \sigma_z \epsilon_z + \tau_{xy} \gamma_{xy} + \tau_{xz} \gamma_{xz} + \tau_{yz} \gamma_{yz}) du dv dk \quad (21)$$

Substituting Equations 22 and 25 into Equation 24 to get the energy equation as:

$$\begin{aligned} \Xi = & \frac{Et^3 \gamma}{24(1+\mu)(1-2\mu)} \int_0^1 \int_0^1 \left[ \left( \frac{\partial \phi_y}{\partial u} \right)^2 \frac{(1-2\mu)}{2} + \frac{1}{\gamma} \frac{\partial \phi_x}{\partial u} * \frac{\partial \phi_y}{\partial v} + \frac{(1-\mu)}{\gamma^2} \left( \frac{\partial \phi_y}{\partial v} \right)^2 + \frac{(1-\mu)}{t^2} * \left( \frac{\partial U}{\partial k} \right)^2 \beta^2 \right. \\ & + \frac{(1-2\mu)}{2\gamma^2} \left( \frac{\partial \phi_x}{\partial v} \right)^2 \\ & + \frac{6(1-2\mu)}{t^2} \left\{ a^2 \phi_x^2 + \left( \frac{\partial U}{\partial u} \right)^2 + a^2 \phi_y^2 + \left( \frac{\partial U}{\partial v} \right)^2 \frac{1}{\gamma^2} + a \left( \frac{\partial U}{\partial u} \right) 2\phi_x + \left( \frac{\partial U}{\partial v} \right) 2a * \frac{\phi_y}{\gamma} \right\} \\ & \left. + \left( \frac{\partial \phi_x}{\partial u} \right)^2 (1-\mu) \right] \partial u \partial v - w\gamma a^2 \int_0^1 \int_0^1 CS \partial u \partial v \quad (22) \end{aligned}$$

## 2.5. Solution to the Equilibrium Equation

The two compatibility equations were obtained by minimizing the total potential energy functional with respect to rotations in x-z and in y-z plane to give:

$$\frac{Et^3 \gamma}{24(1+\mu)(1-2\mu)} \int_0^1 \int_0^1 \left[ 2(1-\mu) \frac{\partial^2 \phi_x}{\partial u^2} + \frac{\partial^2 \phi_y}{\partial u \partial v} * \frac{1}{\gamma} + \frac{(1-2\mu)}{\gamma^2} \frac{\partial^2 \phi_x}{\partial v^2} + \left( 2a^2 \theta_{sx} + 2a \frac{\partial U}{\partial u} \right) \frac{6(1-2\mu)}{t^2} \right] \partial u \partial v = 0 \quad (23)$$

$$\begin{aligned} \frac{Et^3 \gamma}{24(1+\mu)(1-2\mu)} \int_0^1 \int_0^1 \left[ \frac{\partial^2 \phi_x}{\partial u \partial v} * \frac{1}{\gamma} + 2 \frac{\partial^2 \phi_y}{\partial v^2} * \frac{(1-\mu)}{\gamma^2} + 2 \frac{(1-2\mu)}{2} \frac{\partial^2 \phi_y}{\partial u^2} \right. \\ \left. + \left( 2a^2 \phi_y + \frac{2a}{\gamma} \frac{\partial U}{\partial v} \right) \frac{6(1-2\mu)}{t^2} \right] \partial u \partial v = 0 \quad (24) \end{aligned}$$

The solution of the equilibrium differential equation gives the characteristics polynomial displacement and rotation functions as presented in the Equation 25-27 as:

$$U = H_0 \left[ \begin{pmatrix} a_0 \\ a_1 \\ a_2 \\ a_3 \\ a_4 \end{pmatrix} \cdot \begin{pmatrix} 1 & u & u^2 & u^3 & u^4 \end{pmatrix} \right] \cdot \left[ \begin{pmatrix} b_0 \\ b_1 \\ b_2 \\ b_3 \\ b_4 \end{pmatrix} \right] \quad (25)$$

$$\phi_x = \frac{c}{a} \cdot H_0 \left[ \begin{pmatrix} a_1 \\ a_2 \\ a_3 \\ a_4 \end{pmatrix} \cdot \begin{pmatrix} 1 & 2u & 3u^2 & 4u^3 \end{pmatrix} \right] \cdot \left[ \begin{pmatrix} b_0 \\ b_1 \\ b_2 \\ b_3 \\ b_4 \end{pmatrix} \right] \quad (26)$$

$$\phi_y = \frac{c}{a\beta} \cdot H_0 \left[ (1 \ v \ v^2 \ v^3 \ v^4) \begin{bmatrix} a_0 \\ a_1 \\ a_2 \\ a_3 \\ a_4 \end{bmatrix} \cdot (1 \ 2v \ 3v^2 \ 4v^3) \begin{bmatrix} b_1 \\ b_2 \\ b_3 \\ b_4 \end{bmatrix} \right] \tag{27}$$

Considering a transversely loaded rectangular thick plate whose Poisson’s ratio is 0.3 under uniformly distributed load as shown in the Figure 2, the derived trigonometric deflection functions is subjected to a SCFS boundary condition to get the particular solution of the deflection functions is subjected to a SCFS boundary condition to get the particular solution of the deflection.

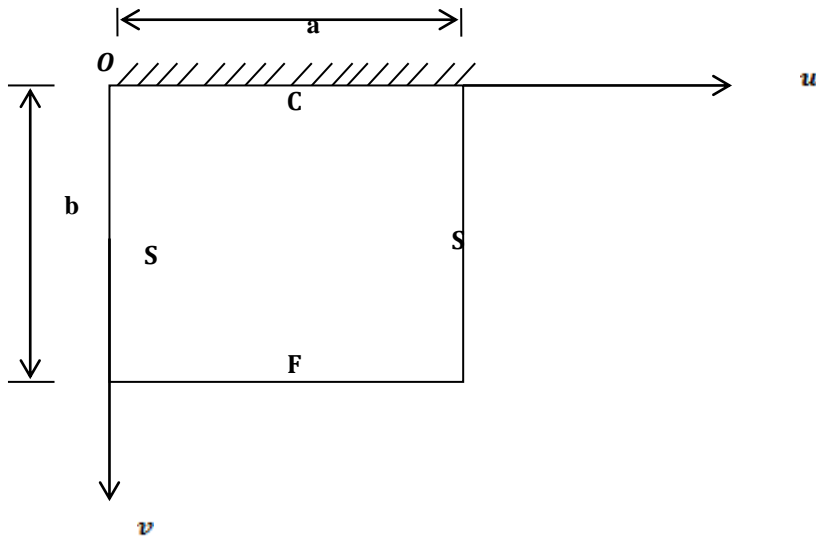


Fig. 2: SCFS rectangular plate

Applying the initial conditions of the plate in Figure 2, the relationship between the displacement and shape function of the plate as:

$$U = C \cdot \eta \tag{28}$$

$$\phi_x = \frac{h}{a} \cdot \frac{\partial C}{\partial u} \tag{29}$$

$$\phi_y = \frac{g}{\gamma a} \cdot \frac{\partial C}{\partial v} \tag{30}$$

The in polynomial form of the shape function of the plate after satisfying the boundary conditions is given as:

$$C = (1.5u^2 - 2.5u + u^4) \times \left( \frac{7v}{3} - \frac{10}{3}v^3 + \frac{10}{3}v^4 - v^5 \right) \tag{31}$$

Substituting Equation 28, 29 and 30 into 22, gives:

$$\begin{aligned} \exists = & \frac{Et^3\gamma}{24(1+\mu)(1-2\mu)} \left[ (1-\mu)h^2r_x + \frac{1}{\gamma^2} \left[ h \cdot g + \frac{(1-2\mu)h^2}{2} + \frac{(1-2\mu)g^2}{2} \right] r_{xy} + \frac{(1-\mu)g^2}{\gamma^4} r_y \right. \\ & \left. + 6(1-2\mu)\beta^2 \left( [h^2 + \eta^2 + 2\eta h] \cdot r_z + \frac{1}{\gamma^2} \cdot [g^2 + \eta^2 + 2\eta g] \cdot r_{2z} \right) - \frac{2qa^4 r_c \eta}{D} \right] \end{aligned} \tag{32}$$

Where:

$$r_x = \int_0^1 \int_0^1 \left( \frac{\partial^2 C}{\partial u^2} \right)^2 \partial u \partial v \quad (33)$$

$$r_{xy} = \int_0^1 \int_0^1 \left( \frac{\partial^2 C}{\partial u \partial v} \right)^2 \partial u \partial v \quad (34)$$

$$r_y = \int_0^1 \int_0^1 \left( \frac{\partial^2 C}{\partial v^2} \right)^2 \partial u \partial v \quad (35)$$

$$r_z = \int_0^1 \int_0^1 \left( \frac{\partial C}{\partial u} \right)^2 \partial u \partial v \quad (36)$$

$$r_{2z} = \int_0^1 \int_0^1 \left( \frac{\partial C}{\partial v} \right)^2 \partial u \partial v \quad (37)$$

$$r_c = \int_0^1 \int_0^1 C \partial u \partial v \quad (38)$$

Minimizing Equation 32 with respect to  $h$  gives:

$$\frac{1}{2\gamma^2} [g + h(1 - 2\mu)] r_{xy} + h r_x (1 - \mu) = -6(1 - 2\mu) \beta^2 [h + \rho] \cdot r_z \quad (39)$$

Minimizing Equation 32 with respect to  $g$  gives:

$$\frac{1}{2\gamma^2} [h + g(1 - 2\mu)] r_{xy} + \frac{(1 - \mu)g}{\gamma^4} k_y = + \frac{6}{\gamma^2} (1 - 2\mu) \beta^2 ([g + \rho] \cdot r_{2z}) \quad (40)$$

Re-write the Equation (39) and (40) and simplifying to give:

$$h = \rho \frac{(k_{12} k_{23} - k_{13} k_{22})}{(k_{12} k_{12} - k_{11} k_{22})} \quad (41)$$

$$g = \rho \frac{(k_{12} k_{13} - k_{11} k_{23})}{(k_{12} k_{12} - k_{11} k_{22})} \quad (42)$$

Where;

$$k_{11} = (1 - \mu) r_x + \frac{1}{2\gamma^2} (1 - 2\mu) r_{xy} + 6(1 - 2\mu) \beta^2 r_z \quad (43)$$

$$k_{12} = k_{21} = \frac{1}{2\gamma^2} r_{xy}; \quad k_{13} = -6(1 - 2\mu) \beta^2 r_z \quad (44)$$

$$k_{22} = \frac{(1 - \mu)}{\gamma^4} r_y + \frac{1}{2\gamma^2} (1 - 2\mu) r_{xy} + \frac{6}{\gamma^2} (1 - 2\mu) \beta^2 r_{2z} \quad (45)$$

$$k_{23} = k_{32} = -\frac{6}{\gamma^2} (1 - 2\mu) \beta^2 r_{2z} \quad (46)$$

Minimizing Equation 32 with respect to  $\rho$  gives:

$$\frac{Et^3\gamma}{24(1+\mu)(1-2\mu)} \left[ 6(1-2\mu)\beta^2 \left( [2\eta+2h].r_z + \frac{1}{\gamma^2}.[2\eta+2g].r_{2z} \right) \right] - \frac{24wa^4r_c(1+\mu)(1-2\mu)}{Et^3} = 0 \tag{47}$$

$$\frac{(1-2\mu)\beta^2Et^3\gamma}{4(1+\mu)(1-2\mu)} \left\{ \left[ \eta + \eta \frac{(k_{12}k_{23} - k_{13}k_{22})}{(k_{12}k_{12} - k_{11}k_{22})} \right].r_z + \frac{1}{\beta^2} \cdot \left[ \eta + \eta \frac{(k_{12}k_{13} - k_{11}k_{23})}{(k_{12}k_{12} - k_{11}k_{22})} \right].r_{2z} \right\} = \frac{wa^4r_c(1+\mu)(1-2\mu)\beta^3}{E} \tag{48}$$

Factorizing Equations (48) and simplifying gives:

$$\eta = \frac{2q(1+\mu)(1-2\mu)\beta^3}{E} \left\{ \frac{ar_c}{(1-2\mu) \left(\frac{\alpha}{t}\right)^2 \left( \left[ 1 + \frac{(k_{12}k_{23} - k_{13}k_{22})}{(k_{12}k_{12} - k_{11}k_{22})} \right].r_z + \frac{1}{\beta^2} \cdot \left[ 1 + \frac{(k_{12}k_{13} - k_{11}k_{23})}{(k_{12}k_{12} - k_{11}k_{22})} \right].r_{2z} \right)} \right\} \tag{49}$$

### 2.6. Exact Displacement and Stress Expression

By substituting the value of  $\eta$  in Equation 49 into Equation 28, the deflection equation after satisfying the boundary condition of SCFS plate is given as:

$$U = \eta (1.5u^2 - 2.5u + u^4) \times \left( \frac{7v}{3} - \frac{10}{3}v^3 + \frac{10}{3}v^4 - v^5 \right) \tag{50}$$

Similarly, the in-plane displacement along x-axis becomes:

$$p = \frac{(k_{12}k_{23} - k_{13}k_{22})}{(k_{12}k_{12} - k_{11}k_{22})} \left\{ \frac{12q(1+\mu)(1-2\mu)\beta^2kr_c}{(1-2\mu) \left(\frac{\alpha}{t}\right)^2 \left( \left[ 1 + \frac{(k_{12}k_{23} - k_{13}k_{22})}{(k_{12}k_{12} - k_{11}k_{22})} \right].r_z + \frac{1}{\beta^2} \cdot \left[ 1 + \frac{(k_{12}k_{13} - k_{11}k_{23})}{(k_{12}k_{12} - k_{11}k_{22})} \right].r_{2z} \right)} \right\} \frac{1}{E} \frac{\partial C}{\partial u} \tag{51}$$

$$p = \frac{12q(1+\mu)(1-2\mu)\beta^2}{E} \left( \frac{kMr_c}{L} \right) \frac{\partial C}{\partial u} \tag{52}$$

Where;

$$L = 6(1-2\mu)\beta^2 \left( [1+h].r_z + \frac{1}{\gamma^2}.[1+g].r_{2z} \right) \tag{53}$$

$$N = \frac{(r_{12}r_{23} - r_{13}r_{22})}{(r_{12}r_{12} - r_{11}r_{22})} \tag{54}$$

$$M = \frac{(r_{12}r_{13} - r_{11}r_{23})}{(r_{12}r_{12} - r_{11}r_{22})} \tag{55}$$

Similarly, the in-plane displacement along y-axis becomes;

$$q = \frac{12q(1+\mu)(1-2\mu)\beta}{E} \left( \frac{kNr_c}{L} \right) \frac{\partial C}{\partial v} \tag{56}$$

The six stress elements after satisfying the boundary condition are presented in Equations (57) – (62) as:

$$\sigma_x = \frac{E}{(1+\mu)(1-2\mu)} \left[ \frac{k}{\beta} \cdot \frac{\partial^2 C}{\partial u^2} (1-\mu) + \mu\beta^4 \cdot \frac{12q(1+\mu)(1-2\mu)}{E} \left( \frac{r_c}{L} \right) \frac{\partial C}{\partial k} + \frac{\mu k}{\gamma\beta} \cdot \frac{\partial^2 C}{\partial v^2} \right] \tag{57}$$

$$\sigma_y = \frac{E}{(1+\mu)(1-2\mu)} \left[ \frac{\mu k}{\beta} \cdot \frac{\partial^2 C}{\partial u^2} + \mu\beta^4 \cdot \frac{12q(1+\mu)(1-2\mu)}{E} \left( \frac{r_c}{L} \right) \frac{\partial C}{\partial k} + \frac{(1-\mu)k}{\gamma\beta} \cdot \frac{\partial^2 C}{\partial v^2} \right] \tag{58}$$

$$\sigma_z = \frac{E}{(1+\mu)(1-2\mu)} \left[ \frac{\mu k}{\beta} \cdot \frac{\partial^2 C}{\partial u^2} + (1-\mu)\beta^4 * \frac{12q(1+\mu)(1-2\mu)}{\beta} \left( \frac{r_c}{L} \right) \frac{\partial C}{\partial k} + \frac{\mu k}{\gamma\beta} \cdot \frac{\partial^2 C}{\partial v^2} \right] \quad (59)$$

$$\tau_{xy} = \frac{E(1-2\mu)}{(1+\mu)(1-2\mu)} \cdot \left[ \frac{k}{2\beta} \cdot \frac{\partial^2 \partial C}{\partial u \partial v} + \frac{\beta^2 k}{2\alpha\gamma} \cdot \frac{12q(1+\mu)(1-2\mu)}{E} \left( \frac{r_c}{L} \right) \frac{\partial^2 \partial C}{\partial u \partial v} \right] \quad (60)$$

$$\tau_{xz} = \frac{(1-2\mu)E}{(1+\mu)(1-2\mu)} \cdot \left[ \frac{1}{2} \frac{\partial C}{\partial u} + \frac{\beta^3}{2} * \frac{12q(1+\mu)(1-2\mu)}{E} \left( \frac{r_c}{L} \right) \frac{\partial C}{\partial u} \right] \quad (61)$$

$$\tau_{yz} = \frac{(1-2\mu)E}{(1+\mu)(1-2\mu)} \cdot \left[ \frac{1}{2} \frac{\partial C}{\partial v} + \frac{\beta^3}{2\gamma} * \frac{12q(1+\mu)(1-2\mu)}{E} \left( \frac{r_c}{L} \right) \frac{\partial C}{\partial v} \right] \quad (62)$$

#### 4. Results and Discussion

The exact polynomial shape-displacement function established was employed to obtain the numerical results of the non-dimensional values for the stresses and displacements of a three-dimensional thick plate with SCFS boundary condition and uniform distributed loading. The outcome of the non-dimensional digits of displacements and stresses for varying span-thickness ratio with length-breadth aspect ratio of 1.0 and 2.0, were presented in figures 3 to 6. The span-depth ratio whose range consists of 4, 5, 10, 15, 20, 50, 100 and CPT, captured thick, moderately thick and thin plates. To determine the bending of the plate at different thickness, this work obtained the non-dimensional figures by expressing the rotation and deflection functions in a polynomial form.

Figures 3 and 4 show that the in-plane displacements (u and v) increases in the negative coordinate while the out-plane displacement (w) decreases in the positive plane as the span-depth ratio increases. The stresses perpendicular to the x and y axis ( $\sigma_x$  and  $\sigma_y$ ) decreased positively and increased in the negative direction respectively, as the span-thickness ratio of the plate increased. The value of the shear stresses in the x-y plane ( $\tau_{xy}$ ) and x-z plane ( $\tau_{xz}$ ) increased negatively with a reduction for the stresses in the y-z plane ( $\tau_{yz}$ ), as the span-depth ratio increased. This decrease was sustained until failure occurred in the plate structure. At a span-thickness ratio between 4 and 20, the value of the deflection varies between 0.0008 and 0.00005, as shown in figure 3. A constant value of 0.00395 was sustained at span-thickness ratio of 50 till 100 which was same with CPT value. It is observed that the difference in deflection is larger when the plate is thicker and it becomes smaller when the span-depth ratio rises under the same loading phenomenon.

For length-breadth aspect ratio of 2.0, figure 3 demonstrates that as the span-thickness ratio gets higher, the non-dimensional values of out-plane displacement (w) reduces with a difference of 0.0009 and 0.0002 span-depth ratio of 4 and 15. A constant deflection value of 0.00480 was found in a span - depth ratio of 15 and 20 while that of 50 and 100 was 0.00470 which is equal to the value obtained for CPT. The values of the in-plane displacements (u and v) dropped as the span-depth ratio rose. The reductions perpetuate until the plate structure deforms outwit the elastic yield stress resulting in structural failure.

Figure 6 represents the outcome of the non-dimensional values of the stresses at varying thickness for length-breadth ratio of 2.0. The normal stress ( $\sigma_x$ ) decreases in the positive coordinate while that of y-axis ( $\sigma_y$ ) increases negatively as the span-thickness ratio gets larger. The value of shear stresses in the x-y plane ( $\tau_{xy}$ ) increased negatively span-depth ratio of 4 and 5 with a negative constant value of 0.0051 a span - depth ratio of 10, 15, 20, 50, 100 and CPT. The value of the shear stress in the x-z plane ( $\tau_{xz}$ ) increased negative for 4 and 5 span-depth ratios, but with a positive reduction for the span-depth ratios ranging from 10 to 100 and CPT. The non-dimensional values of shear stresses in the y-z plane ( $\tau_{yz}$ ) decreased positively for the span-depth ratio of 4 and 5, with a negative decrease for span-thickness ratio between 10 and 100, as well as CPT.

The center deflection obtained in this study was compared to those obtained from 2D shear deformation theory by Onyeka *et al.* [1], as shown in figures 5 and 6. The similarity of these studies is that the non-dimensional deflection values decreased as the span-depth ratio increased. Although both past and current study possess the same behavioral trend as shown the graphs, their disparity is still undeniable as it confirmed that refined plate theories under-estimates and overestimates the bending solution of the plates. The study of Onyeka *et al.* [1] which applied derived shape function produced solutions that were closer to the exact solutions of the present study. While the 2D theories yield approximate solutions, 3-D model as applied in this study offers exact and reliable solutions and should be adopted for an adequate analysis of thick plates. The overall average percentage variation of the deflection values obtained by Onyeka *et al.* [1], is 0.39%. This revealed that at the 99.7 % confidence level, both theory and

methods are identical and applicable for thick plate analysis.

From Table 1, it is shown that the present study predicts slightly higher values of center deflection with highest percentage difference of 5.2%, which occur at span-thickness aspect ratio of 4. The degree of these variations confirms the safety of the current model. The comparative study of the present model as shown in Table 1, clearly confirms that derived deflection function employed in this work is reliably and more accurate as the six stress elements were captured in order to produce an exact solution for the bending problem of plates with SCFS support-order.

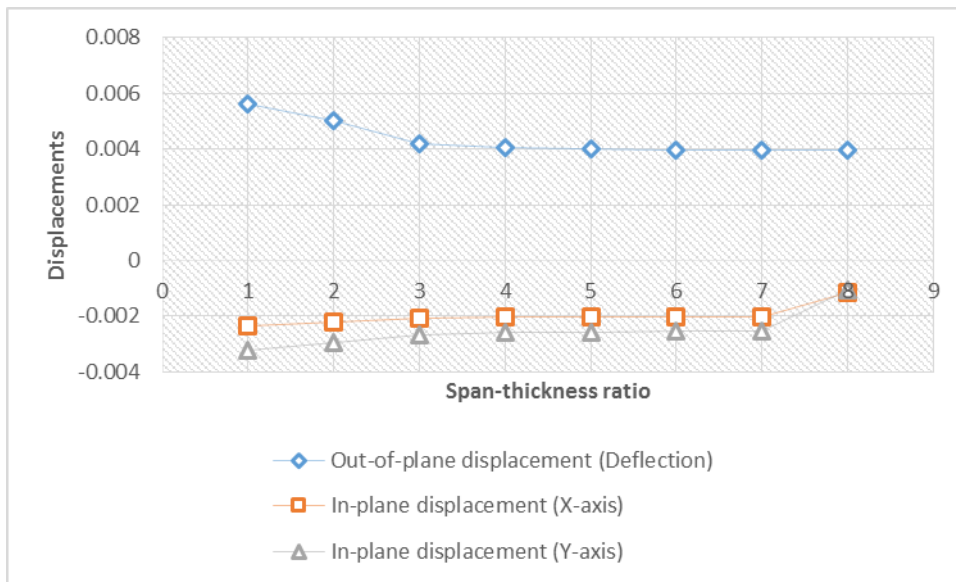


Fig. 3: Displacements and span-thickness ratio variation for SCFS plate with aspect ratio of 1.0

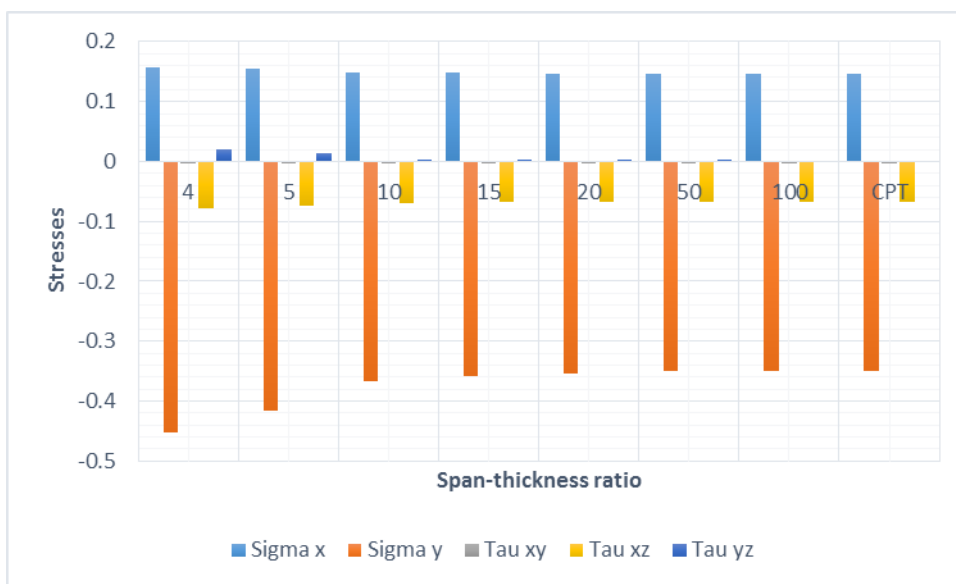


Fig. 4: Stresses and span-thickness ratio variation for SCFS plate with aspect ratio of 1.0

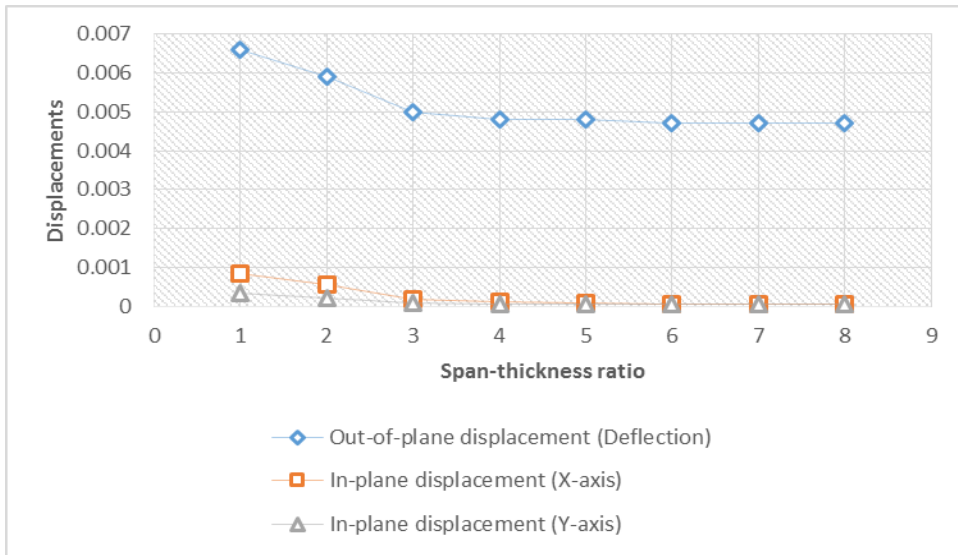


Fig. 5: Displacements and span-thickness ratio variation for SCFS plate with aspect ratio of 2.0

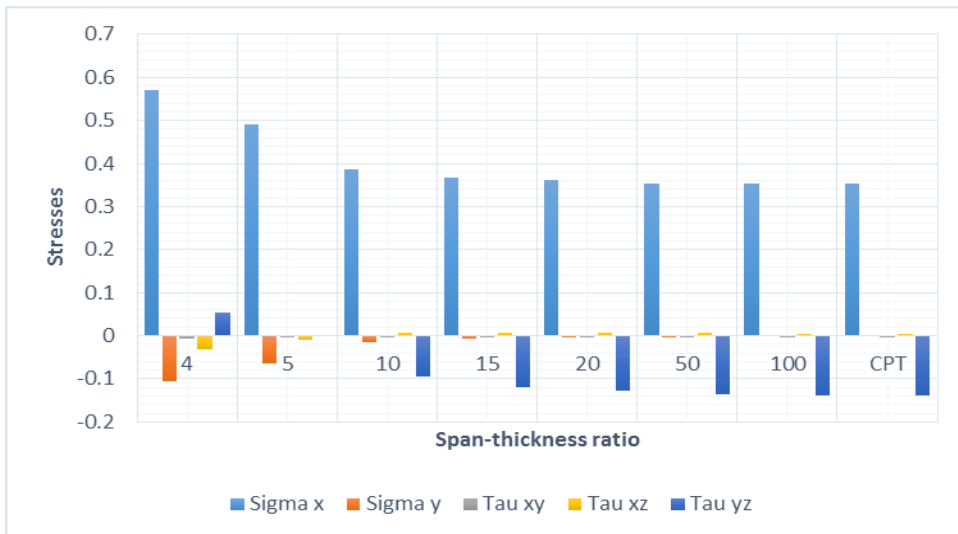


Fig. 6: Stresses and span-thickness ratio variation for SCFS plate with aspect ratio of 2.0

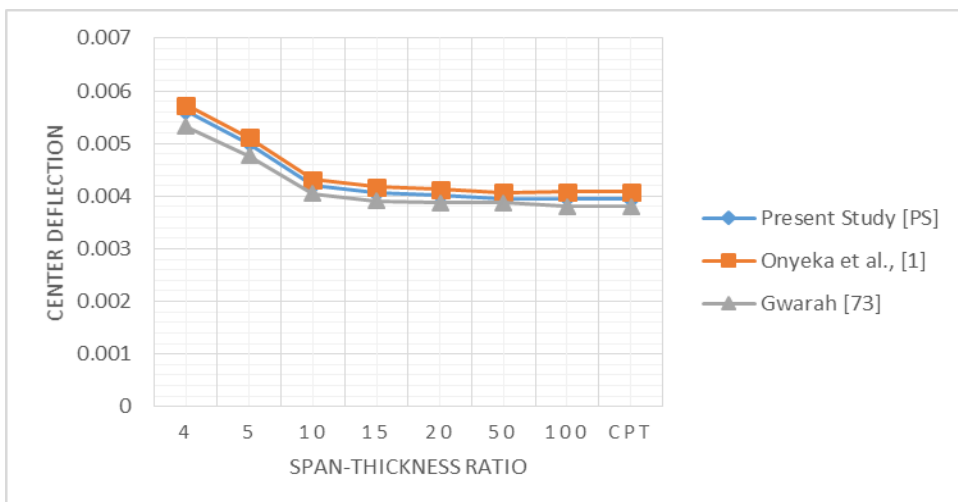


Fig. 7: Comparative center deflection analysis for SCFS square plate at different span-thickness ratio between present study and past studies

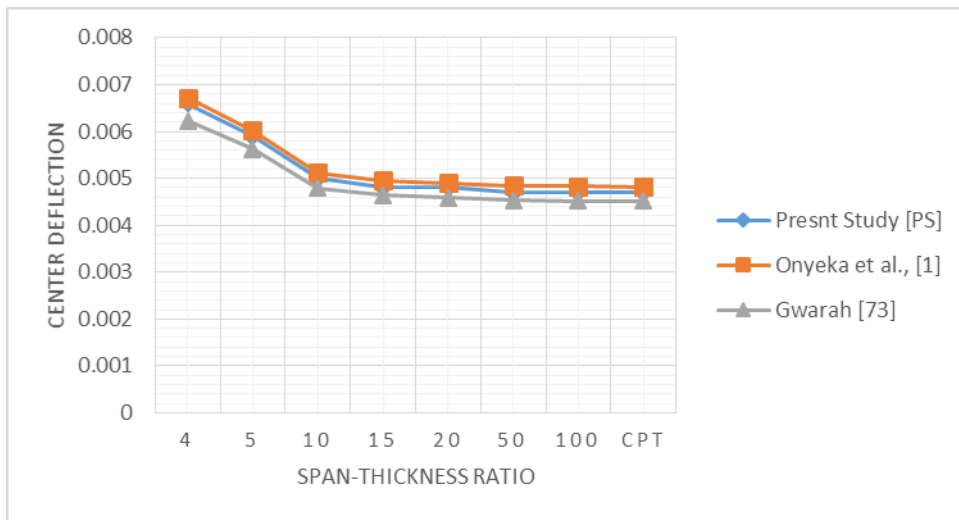


Fig 8: Comparative center deflection analysis for SCFS plate at different span-thickness ratio and length-breadth aspect ratio of 2.0 between present study and past studies

Table 1: Center deflection percentage difference between the present study and past studies for SCFS square plate

Past Scholars	Span-thickness ratio								Average % difference	Overall % difference
	4	5	10	15	20	50	100	CPT		
Onyeka <i>et al.</i> , (2020) [1]	2.1390	2.4000	2.8571	2.9557	2.9925	3.0380	3.2911	3.5533	2.9030	0.3856
Gwarah (2019) [98]	-5.1693	-4.6000	-3.5714	-3.6946	-3.4913	-2.0253	-3.5443	-3.2995	-3.6700	

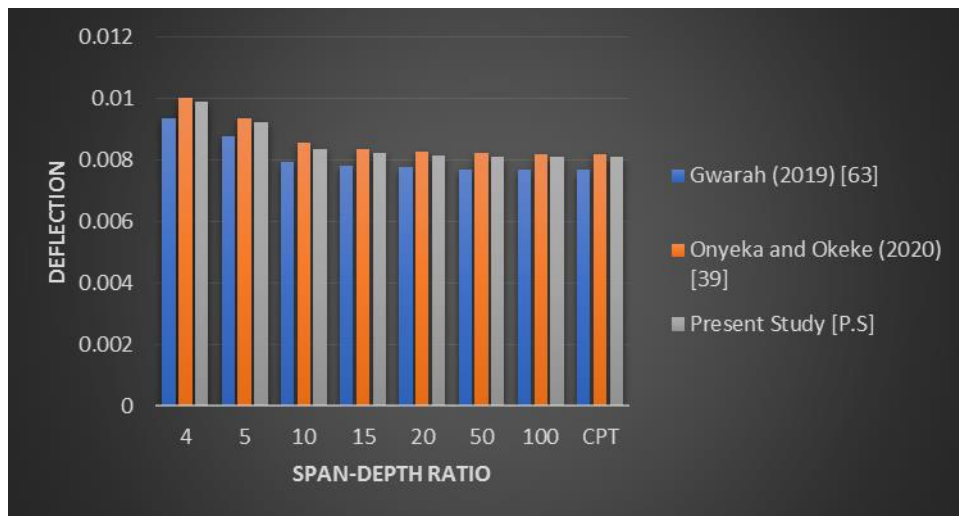


Fig. 7: A graph of deflection against span-depth ratio, comparing previous studies with the present study

### 5. Conclusion

The 3-D elasticity theory has been used to investigate the moments, displacements and stresses of thick rectangular plates with the following conclusions drawn from it:

- The result obtained in this work which are compared with those of previous works revealed that 2-D refined plate theories are quite coarse for thick plate analysis. RPTs under-estimates and over predicts stresses, displacements and bending loads within the engineering allowable error of 3.28% for thick plate analysis.
- The exact polynomial displacement functions offered closed-form solution for thick plate analysis.
- The 3-D elasticity solution gave a more accurate and reliable solution compared refined plate theories and are recommended for the analysis of thick plate under the initial condition.
- The model produced in this study can be employed to analyze plates at varying thicknesses and aspect ratio.

Thus, the model produced in this study can be employed to analyze various categories of the plate.

## Acknowledgements

We would like to acknowledge Ibearugbulem, Owus Mathias of Federal University of Technology, Owerri, Nigeria for providing the technical assistance during this research work.

## References

- [1] O. Festus, E. T. Okeke, W. John, Strain–Displacement expressions and their effect on the deflection and strength of plate, *Advances in Science, Technology and Engineering Systems*, Vol. 5, No. 5, pp. 401-413, 2020.
- [2] F. Onyeka, C. Nwa-David, E. Arinze, Structural imposed load analysis of isotropic rectangular plate carrying a uniformly distributed load using refined shear plate theory, *FUOYE Journal of Engineering and Technology*, Vol. 6, No. 4, pp. 414-419, 2021.
- [3] I. C. Onyechere, O. M. Ibearugbulem, U. Collins Anya, K. Okechukwu Njoku, A. U. Igbojiaku, L. S. Gwarah, The Use of Polynomial Deflection Function in The Analysis of Thick Plates using Higher Order Shear Deformation Theory, *Saudi Journal of Civil Engineering*, Vol. 4, No. 4, pp. 38-46, 2020.
- [4] F. Onyeka, B. Mama, T. Okeke, Exact three-dimensional stability analysis of plate using a direct variational energy method, *Civil Engineering Journal*, Vol. 8, No. 1, pp. 60-80, 2022.
- [5] F. Onyeka, F. Okafor, H. Onah, Application of a new trigonometric theory in the buckling analysis of three-dimensional thick plate, *International Journal of Emerging Technologies*, Vol. 12, No. 1, pp. 228-240, 2021.
- [6] R. Szilard, Theories and applications of plate analysis: classical, numerical and engineering methods, *Appl. Mech. Rev.*, Vol. 57, No. 6, pp. B32-B33, 2004.
- [7] F. Onyeka, O. T. Edozie, Application of higher order shear deformation theory in the analysis of thick rectangular plate, *International Journal on Emerging Technologies*, Vol. 11, No. 5, pp. 62-67, 2020.
- [8] F. Onyeka, T. Okeke, New refined shear deformation theory effect on non-linear analysis of a thick plate using energy method, *Arid Zone Journal of Engineering, Technology and Environment*, Vol. 17, No. 2, pp. 121-140, 2021.
- [9] J. Mantari, A. Oktem, C. G. Soares, A new trigonometric shear deformation theory for isotropic, laminated composite and sandwich plates, *International Journal of Solids and Structures*, Vol. 49, No. 1, pp. 43-53, 2012.
- [10] E. Ventsel, T. Krauthammer, E. Carrera, Thin plates and shells: theory, analysis, and applications, *Appl. Mech. Rev.*, Vol. 55, No. 4, pp. B72-B73, 2002.
- [11] F. Onyeka, Effect of stress and load distribution analysis on an isotropic rectangular plate, *Arid Zone Journal of Engineering, Technology and Environment*, Vol. 17, No. 1, pp. 9-26, 2021.
- [12] J. N. Reddy, 2006, *Theory and analysis of elastic plates and shells*, CRC press,
- [13] F. C. Onyeka, Stability analysis of three-dimensional thick rectangular plate using direct variational energy method, *Journal of Advances in Science and Engineering*, Vol. 6, No. 2, pp. 1-78, 2022.
- [14] S. P. Timoshenko, J. M. Gere, 2009, *Theory of elastic stability*, Courier Corporation,
- [15] F. Onyeka, B. Mama, Analytical study of bending characteristics of an elastic rectangular plate using direct variational energy approach with trigonometric function, *Emerging Science Journal*, Vol. 5, No. 6, pp. 916-928, 2021.
- [16] F. Onyeka, F. Okafor, Buckling solution of a three-dimensional clamped rectangular thick plate using direct variational method, *building structure*, Vol. 1, pp. 3, 2021.
- [17] F. Onyeka, Critical lateral load analysis of rectangular plate considering shear deformation effect, *Global Journal of Civil Engineering*, Vol. 1, pp. 16-27, 2020.
- [18] F. C. Onyeka, T. E. Okeke, Analysis of critical imposed load of plate using variational calculus, *Journal of Advances in Science and Engineering*, Vol. 4, No. 1, pp. 13-23, 2021.
- [19] P. Gujar, K. Ladhane, Bending analysis of simply supported and clamped circular plate, *International Journal of Civil Engineering*, Vol. 2, No. 5, pp. 69-75, 2015.
- [20] G. Kirchhoff, Ueber die Schwingungen einer kreisförmigen elastischen Scheibe, *Annalen der Physik*, Vol. 157, No. 10, pp. 258-264, 1850.
- [21] E. Reissner, The effect of transverse shear deformation on the bending of elastic plates, 1945.

- [22] A. M. Zenkour, Exact mixed-classical solutions for the bending analysis of shear deformable rectangular plates, *Applied Mathematical Modelling*, Vol. 27, No. 7, pp. 515-534, 2003.
- [23] F. Onyeka, T. Okeke, Elastic bending analysis exact solution of plate using alternative i refined plate theory, *Nigerian Journal of Technology*, Vol. 40, No. 6, pp. 1018–1029-1018–1029, 2021.
- [24] A. S. Sayyad, Y. M. Ghugal, Bending and free vibration analysis of thick isotropic plates by using exponential shear deformation theory, *Applied and Computational mechanics*, Vol. 6, No. 1, 2012.
- [25] I. Onyechere, O. Ibearugbulem, U. Anya, L. Anyaogu, C. Awodiji, Free-vibration study of thick rectangular plates using polynomial displacement functions, *Saudi Journal of Engineering and Technology*, Vol. 5, No. 2, pp. 73-80, 2020.
- [26] F. Onyeka, D. Osegbowa, Stress analysis of thick rectangular plate using higher order polynomial shear deformation theory, *FUTO Journal Series–FUTOJNLS*, Vol. 6, No. 2, pp. 142-161, 2020.
- [27] F. Onyeka, D. Osegbowa, E. Arinze, Application of a new refined shear deformation theory for the analysis of thick rectangular plates, *Nigerian Research Journal of Engineering and Environmental Sciences*, Vol. 5, No. 2, pp. 901-917, 2020.
- [28] I. Sayyad, S. Chikalthankar, Bending and free vibration analysis of isotropic plate using refined plate theory, *Bonfring International Journal of Industrial Engineering and Management Science*, Vol. 3, No. 2, pp. 40-46, 2013.
- [29] F. Onyeka, T. Okeke, C. Nwa-David, Static and buckling analysis of a three-dimensional (3-D) rectangular thick plates using exact polynomial displacement function, *European Journal of Engineering and Technology Research*, Vol. 7, No. 2, pp. 29-35, 2022.
- [30] M. Kashtalyan, Three-dimensional elasticity solution for bending of functionally graded rectangular plates, *European Journal of Mechanics-A/Solids*, Vol. 23, No. 5, pp. 853-864, 2004.
- [31] F. Onyeka, B. O. Mama, C. Nwa-David, Application of variation method in three dimensional stability analysis of rectangular plate using various exact shape functions, *Nigerian Journal of Technology*, Vol. 41, No. 1, pp. 8–20-8–20, 2022.
- [32] F. Onyeka, B. Mama, C. Nwa-David, Analytical modelling of a three-dimensional (3D) rectangular plate using the exact solution approach, *IOSR Journal of Mechanical and Civil Engineering*, Vol. 11, No. 1, pp. 10-22, 2022.
- [33] O. F. Chukwudi, O. T. Edozie, N.-D. Chidobere, Buckling Analysis of a Three-Dimensional Rectangular Plates Material Based on Exact Trigonometric Plate Theory, *Journal of Engineering Research and Sciences*, Vol. 1, No. 3, pp. 106-115, 2022.
- [34] F. C. Onyeka, C. D. Nwa-David, T. E. Okeke, Study on Stability Analysis of Rectangular Plates Section Using a Three-Dimensional Plate Theory with Polynomial Function, *Journal of Engineering Research and Sciences*, Vol. 1, No. 4, 2022.
- [35] B. Mama, C. Nwoji, C. Ike, H. Onah, Analysis of simply supported rectangular Kirchhoff plates by the finite Fourier sine transform method, *International Journal of Advanced Engineering Research and Science*, Vol. 4, No. 3, pp. 237109, 2017.
- [36] C. Nwoji, B. Mama, C. Ike, H. Onah, Galerkin-Vlasov method for the flexural analysis of rectangular Kirchhoff plates with clamped and simply supported edges, *IOSR Journal of Mechanical and Civil Engineering*, Vol. 14, No. 2, pp. 61-74, 2017.
- [37] C. Ike, Equilibrium approach in the derivation of differential equations for homogeneous isotropic Mindlin plates, *Nigerian Journal of Technology*, Vol. 36, No. 2, pp. 346-350, 2017.
- [38] N. Osadebe, C. Ike, H. Onah, C. Nwoji, F. Okafor, Application of the Galerkin-Vlasov method to the Flexural Analysis of simply supported Rectangular Kirchhoff Plates under uniform loads, *Nigerian Journal of Technology*, Vol. 35, No. 4, pp. 732-738, 2016.
- [39] Y. M. Ghugal, A. S. Sayyad, A static flexure of thick isotropic plates using trigonometric shear deformation theory, *Journal of Solid Mechanics*, Vol. 2, No. 1, pp. 79-90, 2010.
- [40] J. Mantari, C. G. Soares, Bending analysis of thick exponentially graded plates using a new trigonometric higher order shear deformation theory, *Composite Structures*, Vol. 94, No. 6, pp. 1991-2000, 2012.
- [41] J. C. Ezeh, O. M. Ibearugbulem, L. O. Ettu, L. S. Gwarah, I. C. Onyechere, Application of shear deformation theory for analysis of CCCS and SSFS rectangular isotropic thick plates, *Journal of Mechanical and Civil Engineering (IOSR-JMCE)*, Vol. 15, No. 5, pp. 33-42, 2018.
- [42] D. BHASKAR, A. G. Thakur, I. I. Sayyad, S. V. Bhaskar, Numerical Analysis of Thick Isotropic and Transversely Isotropic Plates in Bending using FE Based New Inverse Shear Deformation Theory, *International Journal of Automotive and Mechanical Engineering*, Vol. 18, No. 3, pp. 8882-8894, 2021.

- [43] O. M. Ibearugbulem, U. C. Onwuegbuchulem, C. Ibearugbulem, Analytical three-dimensional bending analyses of simply supported thick rectangular plate, *International Journal of Engineering Advanced Research*, Vol. 3, No. 1, pp. 27-45, 2021.
- [44] A. Y. Grigorenko, A. Bergulev, S. Yaremchenko, Numerical solution of bending problems for rectangular plates, *International Applied Mechanics*, Vol. 49, pp. 81-94, 2013.
- [45] F. Onyeka, T. Okeke, B. Mama, Static Elastic Bending Analysis of a Three-Dimensional Clamped Thick Rectangular Plate using Energy Method, *HighTech and Innovation Journal*, Vol. 3, No. 3, pp. 267-281, 2022.
- [46] M. Mohammadi, A. Farajpour, A. Moradi, M. Hosseini, Vibration analysis of the rotating multilayer piezoelectric Timoshenko nanobeam, *Engineering Analysis with Boundary Elements*, Vol. 145, pp. 117-131, 2022.
- [47] M. Mohammadi, A. Rastgoo, Primary and secondary resonance analysis of FG/lipid nanoplate with considering porosity distribution based on a nonlinear elastic medium, *Mechanics of Advanced Materials and Structures*, Vol. 27, No. 20, pp. 1709-1730, 2020.
- [48] M. Mohammadi, M. Hosseini, M. Shishesaz, A. Hadi, A. Rastgoo, Primary and secondary resonance analysis of porous functionally graded nanobeam resting on a nonlinear foundation subjected to mechanical and electrical loads, *European Journal of Mechanics-A/Solids*, Vol. 77, pp. 103793, 2019.
- [49] M. Mohammadi, A. Rastgoo, Nonlinear vibration analysis of the viscoelastic composite nanoplate with three directionally imperfect porous FG core, *Structural Engineering and Mechanics, An Int'l Journal*, Vol. 69, No. 2, pp. 131-143, 2019.
- [50] A. Farajpour, A. Rastgoo, M. Mohammadi, Vibration, buckling and smart control of microtubules using piezoelectric nanoshells under electric voltage in thermal environment, *Physica B: Condensed Matter*, Vol. 509, pp. 100-114, 2017.
- [51] A. Farajpour, M. H. Yazdi, A. Rastgoo, M. Loghmani, M. Mohammadi, Nonlocal nonlinear plate model for large amplitude vibration of magneto-electro-elastic nanoplates, *Composite Structures*, Vol. 140, pp. 323-336, 2016.
- [52] A. Farajpour, M. H. Yazdi, A. Rastgoo, M. Mohammadi, A higher-order nonlocal strain gradient plate model for buckling of orthotropic nanoplates in thermal environment, *Acta Mechanica*, Vol. 227, pp. 1849-1867, 2016.
- [53] M. Mohammadi, M. Safarabadi, A. Rastgoo, A. Farajpour, Hygro-mechanical vibration analysis of a rotating viscoelastic nanobeam embedded in a visco-Pasternak elastic medium and in a nonlinear thermal environment, *Acta Mechanica*, Vol. 227, pp. 2207-2232, 2016.
- [54] M. R. Farajpour, A. Rastgoo, A. Farajpour, M. Mohammadi, Vibration of piezoelectric nanofilm-based electromechanical sensors via higher-order non-local strain gradient theory, *Micro & Nano Letters*, Vol. 11, No. 6, pp. 302-307, 2016.
- [55] M. Baghani, M. Mohammadi, A. Farajpour, Dynamic and stability analysis of the rotating nanobeam in a nonuniform magnetic field considering the surface energy, *International Journal of Applied Mechanics*, Vol. 8, No. 04, pp. 1650048, 2016.
- [56] M. Goodarzi, M. Mohammadi, M. Khooran, F. Saadi, Thermo-mechanical vibration analysis of FG circular and annular nanoplate based on the visco-pasternak foundation, *Journal of Solid Mechanics*, Vol. 8, No. 4, pp. 788-805, 2016.
- [57] H. Asemi, S. Asemi, A. Farajpour, M. Mohammadi, Nanoscale mass detection based on vibrating piezoelectric ultrathin films under thermo-electro-mechanical loads, *Physica E: Low-dimensional Systems and Nanostructures*, Vol. 68, pp. 112-122, 2015.
- [58] M. Safarabadi, M. Mohammadi, A. Farajpour, M. Goodarzi, Effect of surface energy on the vibration analysis of rotating nanobeam, 2015.
- [59] M. Goodarzi, M. Mohammadi, A. Gharib, Techno-Economic Analysis of Solar Energy for Cathodic Protection of Oil and Gas Buried Pipelines in Southwestern of Iran, in *Proceeding of*, [https://publications.waset.org/abstracts/33008/techno-economic-analysis-of ...](https://publications.waset.org/abstracts/33008/techno-economic-analysis-of-...), pp.
- [60] M. Mohammadi, A. A. Nekounam, M. Amiri, The vibration analysis of the composite natural gas pipelines in the nonlinear thermal and humidity environment, in *Proceeding of*, <https://civilica.com/doc/540946/>, pp.
- [61] M. Goodarzi, M. Mohammadi, M. Rezaee, Technical Feasibility Analysis of PV Water Pumping System in Khuzestan Province-Iran, in *Proceeding of*, [https://publications.waset.org/abstracts/18930/technical-feasibility ...](https://publications.waset.org/abstracts/18930/technical-feasibility-...), pp.
- [62] M. Mohammadi, A. Farajpour, A. Moradi, M. Ghayour, Shear buckling of orthotropic rectangular graphene sheet embedded in an elastic medium in thermal environment, *Composites Part B: Engineering*, Vol. 56, pp. 629-637, 2014.

- [63] M. Mohammadi, A. Moradi, M. Ghayour, A. Farajpour, Exact solution for thermo-mechanical vibration of orthotropic mono-layer graphene sheet embedded in an elastic medium, *Latin American Journal of Solids and Structures*, Vol. 11, pp. 437-458, 2014.
- [64] M. Mohammadi, A. Farajpour, M. Goodarzi, F. Dinari, Thermo-mechanical vibration analysis of annular and circular graphene sheet embedded in an elastic medium, *Latin American Journal of Solids and Structures*, Vol. 11, pp. 659-682, 2014.
- [65] M. Mohammadi, A. Farajpour, M. Goodarzi, Numerical study of the effect of shear in-plane load on the vibration analysis of graphene sheet embedded in an elastic medium, *Computational Materials Science*, Vol. 82, pp. 510-520, 2014.
- [66] A. Farajpour, A. Rastgoo, M. Mohammadi, Surface effects on the mechanical characteristics of microtubule networks in living cells, *Mechanics Research Communications*, Vol. 57, pp. 18-26, 2014.
- [67] S. R. Asemi, M. Mohammadi, A. Farajpour, A study on the nonlinear stability of orthotropic single-layered graphene sheet based on nonlocal elasticity theory, *Latin American Journal of Solids and Structures*, Vol. 11, pp. 1541-1546, 2014.
- [68] M. Goodarzi, M. Mohammadi, A. Farajpour, M. Khooran, Investigation of the effect of pre-stressed on vibration frequency of rectangular nanoplate based on a visco-Pasternak foundation, 2014.
- [69] S. Asemi, A. Farajpour, H. Asemi, M. Mohammadi, Influence of initial stress on the vibration of double-piezoelectric-nanoplate systems with various boundary conditions using DQM, *Physica E: Low-dimensional Systems and Nanostructures*, Vol. 63, pp. 169-179, 2014.
- [70] S. Asemi, A. Farajpour, M. Mohammadi, Nonlinear vibration analysis of piezoelectric nanoelectromechanical resonators based on nonlocal elasticity theory, *Composite Structures*, Vol. 116, pp. 703-712, 2014.
- [71] M. Mohammadi, M. Ghayour, A. Farajpour, Free transverse vibration analysis of circular and annular graphene sheets with various boundary conditions using the nonlocal continuum plate model, *Composites Part B: Engineering*, Vol. 45, No. 1, pp. 32-42, 2013.
- [72] M. Mohammadi, M. Goodarzi, M. Ghayour, A. Farajpour, Influence of in-plane pre-load on the vibration frequency of circular graphene sheet via nonlocal continuum theory, *Composites Part B: Engineering*, Vol. 51, pp. 121-129, 2013.
- [73] M. Mohammadi, A. Farajpour, M. Goodarzi, R. Heydarshenas, Levy type solution for nonlocal thermo-mechanical vibration of orthotropic mono-layer graphene sheet embedded in an elastic medium, *Journal of Solid Mechanics*, Vol. 5, No. 2, pp. 116-132, 2013.
- [74] M. Mohammadi, A. Farajpour, M. Goodarzi, H. Mohammadi, Temperature Effect on Vibration Analysis of Annular Graphene Sheet Embedded on Visco-Pasternak Foundati, *Journal of Solid Mechanics*, Vol. 5, No. 3, pp. 305-323, 2013.
- [75] M. Danesh, A. Farajpour, M. Mohammadi, Axial vibration analysis of a tapered nanorod based on nonlocal elasticity theory and differential quadrature method, *Mechanics Research Communications*, Vol. 39, No. 1, pp. 23-27, 2012.
- [76] A. Farajpour, A. Shahidi, M. Mohammadi, M. Mahzoon, Buckling of orthotropic micro/nanoscale plates under linearly varying in-plane load via nonlocal continuum mechanics, *Composite Structures*, Vol. 94, No. 5, pp. 1605-1615, 2012.
- [77] M. Mohammadi, M. Goodarzi, M. Ghayour, S. Alivand, Small scale effect on the vibration of orthotropic plates embedded in an elastic medium and under biaxial in-plane pre-load via nonlocal elasticity theory, 2012.
- [78] A. Farajpour, M. Mohammadi, A. Shahidi, M. Mahzoon, Axisymmetric buckling of the circular graphene sheets with the nonlocal continuum plate model, *Physica E: Low-dimensional Systems and Nanostructures*, Vol. 43, No. 10, pp. 1820-1825, 2011.
- [79] A. Farajpour, M. Danesh, M. Mohammadi, Buckling analysis of variable thickness nanoplates using nonlocal continuum mechanics, *Physica E: Low-dimensional Systems and Nanostructures*, Vol. 44, No. 3, pp. 719-727, 2011.
- [80] H. Moosavi, M. Mohammadi, A. Farajpour, S. Shahidi, Vibration analysis of nanorings using nonlocal continuum mechanics and shear deformable ring theory, *Physica E: Low-dimensional Systems and Nanostructures*, Vol. 44, No. 1, pp. 135-140, 2011.
- [81] M. Mohammadi, M. Ghayour, A. Farajpour, Analysis of free vibration sector plate based on elastic medium by using new version differential quadrature method, *Journal of solid mechanics in engineering*, Vol. 3, No. 2, pp. 47-56, 2011.

- [82] A. Farajpour, M. Mohammadi, M. Ghayour, Shear buckling of rectangular nanoplates embedded in elastic medium based on nonlocal elasticity theory, in *Proceeding of*, [www.civilica.com/Paper-ISME19-ISME19\\_390.html](http://www.civilica.com/Paper-ISME19-ISME19_390.html), pp. 390.
- [83] M. Mohammadi, A. Farajpour, A. R. Shahidi, Higher order shear deformation theory for the buckling of orthotropic rectangular nanoplates using nonlocal elasticity, in *Proceeding of*, [www.civilica.com/Paper-ISME19-ISME19\\_391.html](http://www.civilica.com/Paper-ISME19-ISME19_391.html), pp. 391.
- [84] M. Mohammadi, A. Farajpour, A. R. Shahidi, Effects of boundary conditions on the buckling of single-layered graphene sheets based on nonlocal elasticity, in *Proceeding of*, [www.civilica.com/Paper-ISME19-ISME19\\_382.html](http://www.civilica.com/Paper-ISME19-ISME19_382.html), pp. 382.
- [85] M. Mohammadi, M. Ghayour, A. Farajpour, Using of new version integral differential method to analysis of free vibration orthotropic sector plate based on elastic medium, in *Proceeding of*, [www.civilica.com/Paper-ISME19-ISME19\\_497.html](http://www.civilica.com/Paper-ISME19-ISME19_497.html), pp. 497.
- [86] M. Zamani Nejad, A. Hadi, Eringen's non-local elasticity theory for bending analysis of bi-directional functionally graded Euler–Bernoulli nano-beams, *International Journal of Engineering Science*, Vol. 106, pp. 1-9, 2016.
- [87] M. Z. Nejad, A. Hadi, Non-local analysis of free vibration of bi-directional functionally graded Euler–Bernoulli nano-beams, *International Journal of Engineering Science*, Vol. 105, pp. 1-11, 2016.
- [88] M. Mohammadi, A. Farajpour, A. Rastgoo, Coriolis effects on the thermo-mechanical vibration analysis of the rotating multilayer piezoelectric nanobeam, *Acta Mechanica*, Vol. 234, No. 2, pp. 751-774, 2023/02/01, 2023.